

Biotechnic & Histochemistry

ISSN: (Print) (Online) Journal homepage: https://www.tandfonline.com/loi/ibih20

Expression of nuclear factor-erythroid 2-related factor 2 (Nrf2) in mouse uterus during the peri-implantation period

Hakan Soylu, Kubra Aksu, Ezgi Golal, Ismail Ustunel, V. Nimet Izgut-Uysal & Nuray Acar

To cite this article: Hakan Soylu, Kubra Aksu, Ezgi Golal, Ismail Ustunel, V. Nimet Izgut-Uysal & Nuray Acar (2022): Expression of nuclear factor-erythroid 2-related factor 2 (Nrf2) in mouse uterus during the peri-implantation period, Biotechnic & Histochemistry, DOI: 10.1080/10520295.2022.2127156

To link to this article: https://doi.org/10.1080/10520295.2022.2127156

Published online: 17 Oct 2022.

Submit your article to this journal

Article views: 55

View related articles

View Crossmark data

Full Terms & Conditions of access and use can be found at
https://www.tandfonline.com/action/journalInformation?journalCode=ibih20

BIOTECHNIC & HISTOCHEMISTRY
https://doi.org/10.1080/10520295.2022.2127156

Taylor & Francis
Taylor & Francis Group

Check for updates

Expression of nuclear factor-erythroid 2-related factor 2 (Nrf2) in mouse uterus during the peri-implantation period

Hakan Soylu[a], Kubra Aksu[b], Ezgi Golal[b], Ismail Ustunel[b], V. Nimet Izgut-Uysal[b,c], and Nuray Acar [b]

[a]Department of Histology and Embryology, Faculty of Medicine, Duzce University, Duzce, Turkey; [b]Department of Histology and Embryology, Faculty of Medicine, Akdeniz University, Antalya, Turkey; [c]Department of Physiology, Faculty of Medicine, Akdeniz University, Antalya, Turkey

ABSTRACT

Nuclear factor-erythroid 2-related factor- 2 (Nrf2) is a nuclear transcription factor that facilitates transcription of genes for detoxification enzymes and antioxidant proteins. We investigated the distribution and expression of Nrf2 during the peri-implantation period. We detected Nrf2 in uteri of mice during estrus (control) and on days 1, 4, 5, 6 and 8 of pregnancy using immunohistochemistry, quantitative real-time polymerase chain reaction and western blotting. Nrf2 immunostaining was significantly greater on days 1, 5 and 6 of pregnancy compared to controls, and on days 4 and 8 of pregnancy; western blotting results were consistent with immunohistochemical observations. Nrf2 mRNA levels on days 5 and 8 were significantly higher than for control uteri. Increased expression of Nrf2 on days 1, 5 and 6 of pregnancy may be important for uterine receptivity, implantation and decidualization by protecting the developing embryo and uterus from the adverse effects of oxidative stress.

KEYWORDS

Mouse, Nrf2; pregnancy; reactive oxygen species; uterus

Implantation in mammals requires synchronous activity between the blastocyst and the uterine endometrium (Dey et al. 2004; Wang and Dey 2006). Uterine sensitivity consists of pre-receptive, receptive and nonreceptive phases (Dey et al. 2004). Implantation occurs when the blastocyst interacts physically and physiologically with the uterine endometrium during the receptive phase. Implantation exhibits three stages: apposition, adhesion and penetration (Enders and Schlafke 1969). During apposition, the blastocyst contacts the endometrial epithelium at the implantation site. This is followed by adhesion in which blastocyst trophoblast cells attach to the uterine luminal epithelium. Penetration occurs when invasive trophoblast cells pass through the basement membrane of the endometrial epithelium and invade the stroma (Bischof and Campana 1997). Localized endometrial vascular permeability, which is restricted to the blastocyst region, is coincident in mice with the attachment phase and occurs on the evening of day 4 (Das et al. 1994); the process is more evident on day 5. On day 6, uterine stromal cells are in direct contact with the blastocyst. Altered early implantation causes either pregnancy failure or late stage pregnancy defects (Wang and Dey 2006; Cha et al. 2012).

Cell type-specific proliferation and differentiation during the pre-implantation period are regulated by steroid hormones in the mouse uterus (Martin and Finn 1968; Huet-Hudson et al. 1989). Preovulatory ovarian estrogen controls epithelial cell proliferation on days 1 and 2 of pregnancy. On day 3 of pregnancy, progesterone from the corpus luteum stimulates proliferation of stromal cells. Proliferation of these cells is enhanced by pre-implantation estrogen secretion at the beginning of day 4. Stromal cells proliferate and differentiate into decidual cells during implantation (Martin and Finn 1968; Psychoyos 1973; Huet-Hudson et al. 1989). Increased endometrial vascular permeability at the site of the blastocyst is the earliest sign of initiation of implantation in rodents (Psychoyos 1973; Huet and Dey 1987; Paria et al. 1993). Increased endometrial vascular permeability occurs simultaneously with the first attachment reaction (Enders 1967). The attachment reaction in the mouse occurs during the evening of day 4 of pregnancy (Das et al. 1994). After attachment, decidualization of the stromal cells and apoptosis of the luminal epithelial cells are observed at the blastocyst implantation site (Parr et al. 1988).

In the mouse, the primary decidual zone (PDZ) is formed by differentiation of stromal cells at the site of blastocyst during the afternoon of day 5. The PDZ is epithelioid and avascular (Paria et al. 1999). By day 6,

CONTACT Nuray Acar nurayacar@akdeniz.edu.tr Department of Histology and Embryology, Faculty of Medicine, Akdeniz University, Antalya, 07070, Turkey

© 2022 The Biological Stain Commission

the stromal cells adjacent to the PDZ continue to proliferate and differentiate to form polyploid decidual cells, which constitute a secondary decidual zone (SDZ) around the PDZ. While completing the development of the SDZ by day 7 of pregnancy, the PDZ gradually degenerates by apoptosis and most of these cells disappear by day 8 of pregnancy. After day 8, placental and embryonic growth slowly replaces the SDZ (Das 2010).

Nuclear factor-erythroid 2-related factor 2 (Nrf2) is a member of the 'cap-*n*-collar' class of basic leucine zipper transcription factors. Nrf2 is a transcription factor in the nucleus that provides coordinated activation of cytoprotective genes including biotransformation enzymes, antioxidant proteins, drug carriers, anti-apoptotic proteins and proteasomes (Zhang 2006; Kwak et al. 2007; Kaspar et al. 2009). Nrf2 is expressed in all cell types and is important for antioxidant response (Ikeda et al. 2004; Rojo de la Vega et al. 2018). Nrf2 generally is present at a low basal level that is regulated by Keap1 by ubiquitination and proteasomal degradation (Itoh et al. 1999). Chemical preservatives, such as sulforaphane, stabilize Nrf2 and prevent its degradation so that NRF2 can be translocated to the nucleus to activate the antioxidant response (Lee and Surh 2005). Therefore, the level of Nrf2 is increased and the Nrf2-mediated antioxidant response is activated. Nrf2 knockout mice do not exhibit phenotypic defects, but are susceptible to oxidative stress (Ramos-Gomez et al. 2001).

Decreased antioxidant capacity causes increased reactive oxygen species (ROS), which cause oxidative stress. ROS are a by-product of mitochondrial respiration (Ruder et al. 2009). Appropriate physiological levels of ROS are required for effective functioning of various biological pathways and for maintaining homeostasis. Low levels of free radicals regulate female reproductive activities including oocyte maturation, ovulation, follicular atresia, luteal regression, fertilization and formation of corpora lutea (Riley and Behrman 1991). Increased levels of superoxide anion in the mouse uterus on day 5 of pregnancy may contribute to vascular permeability at the beginning of implantation (Laloraya et al. 1989a, 1989b). NADPH-dependent superoxide anion production is increased in the uterus and ovaries of mice during early pregnancy and during the estrous cycle (Jain et al. 2000). Robust antioxidant enzyme systems prior to implantation are essential to create a receptive uterine endometrium for embryonic development (Blomberg et al. 2005).

Although the roles of antioxidants in the uterus during pregnancy have been described (Laloraya et al. 1989a, 1989b; Riley and Behrman 1991; Jain et al. 2000; Blomberg et al. 2005), the role of Nrf2 in the mouse uterus during the peri-implantation period has not been reported. We investigated the immunolocalization, and mRNA and protein levels of Nrf2 in the mouse uterus during the peri-implantation period.

Material and methods

Experimental protocol

Our protocol was consistent with the Helsinki and International Association for the study of pain guidelines and was approved by the Animal Care and Usage Committee of Akdeniz University, approval no. 2013.10.04.

We used 60 6–8-week-old female and 20 male Balb/C mice obtained from the Experimental Animals Unit of Akdeniz University. The mice were housed at 24 ± 2 °C and 50 ± 5% humidity with a 12 h light:12 h dark cycle and provided food and water *ad libitum*. Two or three female mice were housed with a male mouse overnight for mating; the females were checked for vaginal plugs next morning and presence of vaginal plugs was defined as day 1 of pregnancy.

We established six experimental groups of 10 animals: group D1, day 1 of pregnancy; D4, day 4 of pregnancy; D5, day 5 of pregnancy; D6, day 6 of pregnancy; D8, day 8 of pregnancy; group C, control group consisting of nonpregnant females in estrus. On the appropriate days, mice were sacrificed by cervical dislocation following anesthesia using 8 mg ketamine and 1.2 mg xylazine in 0.1 ml H_2O/10 g body weight (Sigma Aldrich, St. Louis, MO) and uteri or implantation sites were collected. For group C, vaginal smears were taken and stained with 0.1% (w/v) aqueous crystal violet (Merck, Darmstadt, Germany) to determine the estrus phase. Mice with vaginal smears containing large anucleate squamous epithelial cells, which characterize estrus, were included in group C. The mice in group C were sacrificed as above. For the D1 and D4 groups, pregnancy was confirmed by recovering embryos from the oviducts and uterus, respectively. For the D5 and D6 groups, implantation sites were identified by intravenous injection of 0.1 ml 1% (w/v) Chicago blue (Sigma Aldrich) in saline into the tail vein, after which implantation sites were demarcated by discrete blue bands owing to increased capillary permeability in the implantation sites, which enables Chicago blue to bind to serum proteins and accumulate in the implantation sites. For the D8 group, implantation sites were visible without Chicago blue

injection. Some uteri and implantation sites of sacrificed mice were preserved in liquid nitrogen for western blot study, while others were fixed with 10% formalin (Merck) for immunohistochemical staining.

Tissue processing

Excised uteri and implantation sites were fixed with 10% formalin at room temperature for approximately 24 h, washed with running tap water for 3 h, dehydrated through 70, 80 and 90% ethanol for 24 h each and 4 h in 100% ethanol. Tissues were cleared with xylene (Sigma Aldrich) for approximately 4 min and embedded in paraffin wax (Merck).

Immunohistochemistry

Formalin fixed paraffin embedded sections were cut at 5 µm and placed on electrostatically charged slides (Thermo Scientific). Mounted sections were placed in an incubator at 56 °C overnight to facilitate deparaffinization and adhesion of the tissues to the slides. For immunostaining, sections were deparaffinized with xylene and rehydrated through a graded ethanol series. Antigen retrieval was performed by treating the samples three times with 10 mM citrate buffer, pH 6.0 (Merck), in a microwave oven at 750 W for 5 min to expose target proteins masked by the fixative. After cooling for 20 min at room temperature, sections were washed with phosphate buffered saline, pH 7.4, (PBS) for 5 min. Endogenous peroxidase activity was blocked by incubation in methanol containing 3% (v/v) H_2O_2 (Merck) for 30 min, then washed three times with PBS. Sections were incubated with Ultra UVBlock TA- 125UB blocking solution (LabVision Corp., Fremont, CA) for 7 min at room temperature to block nonspecific binding. Excess serum was drained and sections were incubated at 4 °C overnight with rabbit polyclonal anti-Nrf2 antibody (Santa Cruz Biotechnology, Santa Cruz, CA) diluted 1:100. The primary antibody was substituted with rabbit IgG (Santa Cruz Biotechnology) at the same dilution as Nrf2 as a negative control. On the following day, after washing out the primary antibody with PBS, sections were incubated with a biotinylated anti-rabbit secondary antibody (BA- 1000; Vector Laboratories, Burlingame, CA) diluted 1:500 for 45 min at room temperature followed by incubation with horseradish peroxidase-conjugated streptavidin (Thermo Scientific) for 30 min at room temperature. All incubation steps were performed in a humidified chamber to avoid dehydration of the sections. After sections were washed in PBS, peroxidase activity was visualized using 3,3 diaminobenzidine (DAB) (Sigma Aldrich) for 2 min. Sections were counterstained with Mayer's hematoxylin (Merck), then mounted with Kaiser's glycerin gelatin (Merck). Sections were inspected and photographed using an Axioplan 100 light microscope (Zeiss, Jena, Germany).

We evaluated immunohistochemical staining of Nrf2 during the peri-implantation period in uterus and implantation sites using the Image J Version 1.36b image analysis software (National Institutes of Health, Bethesda, MD). Photographs of six different areas for each slide were taken at 400 x magnification. In each photograph, the staining intensity of the total area, including hematoxylin and DAB, was determined at the appropriate threshold using Image J. Then, the staining intensity of only the DAB positive area was measured. The staining percentage was obtained by dividing the staining intensity of the DAB positive area by the total staining intensity and multiplying by 100.

Western blotting

Tissue samples for each experimental group were weighed, then placed in homogenization buffer supplemented with complete protease inhibitor cocktail (Merck). Following homogenization, samples were centrifuged at 10,000 x g for 10 min. Supernatants were collected and stored at −80 °C. Protein concentrations were determined using a standard bicinchoninic acid assay with bicinchoninic acid solution and copper(II) sulfate solution (Sigma Aldrich). Samples were heated for 5 min at 95 °C, and 50 µg protein was applied to each lane of electrophoresis gels. Samples then were subjected to sodium dodecyl sulfate-polyacrylamide gel electrophoresis under standard conditions (Acar et al. 2019). Separated proteins were transferred onto polyvinylidene difluoride membranes (Bio-Rad, Hercules, CA) in a buffer containing 0.2 mol/l glycine (Bio-Rad), 25 mM Tris (Merck) and 20% (v/v) methanol, overnight at 4 °C. After blocking with 5% (w/v) nonfat dry milk (Sigma Aldrich), membranes were incubated with rabbit polyclonal anti-Nrf2 (Santa Cruz Biotechnology) diluted 1:200 overnight at 4 °C. After washing, membranes were incubated for 1 h at room temperature with horseradish peroxidase-conjugated secondary anti-rabbit IgG diluted 1:2000 (Vector Laboratories). The reaction was visualized using chemiluminescence based Super Signal CL HRP Substrate System (Thermo Fisher Scientific, Rockford, IL) and the membranes were exposed to Hyperfilm

(Amersham Hyperfilm ECL, GE Healthcare, Buckinghamshire, UK). The film was processed using a developer (Ilford Photo, Cheshire, UK) and fixative (Ilford Photo), then washed with distilled water and dried. Membranes also were labeled using an identical protocol for binding a rabbit monoclonal anti-beta actin antibody diluted 1:5000, (Cell Signaling, Danvers, MA) as an internal control to confirm the equal loading of the samples. The bands were quantified using Image J Version 1.36b image analysis software. The bands obtained were scanned and transferred to the computer. The image was opened in the ImageJ program and the bands were selected individually using the frame selection tool. Band analysis was performed using the Analyze > Gels > Plot Lanes tabs, respectively, and the profile plot of the band within each rectangle was obtained. The base parts of each profile plot were joined by a straight line. The wand tool was selected from Image J toolbar and measurements were opened in the results window by clicking on each constrained profile plot. These procedures were applied to both Nrf2 and beta actin. The Nrf2 protein expression level was determined as a proportion of the Nrf2 to beta actin.

Quantitative real-time polymerase chain reaction (qRT-PCR)

Total RNA was isolated from uteri and implantation sites using trizol reagent (Invitrogen, Carlsbad, CA) according to the manufacturer's instructions. RNA concentration was quantified by measuring the absorbance at 260 and 280 nm. Isolated RNA was treated with DNase I (Ambion, Buckinghamshire, UK) to eliminate DNA contamination. We prepared cDNA from 2 µg total RNA using the SuperScript III First-Strand Synthesis System for RT-PCR (Invitrogen) according to the manufacturer's instructions.

PCR amplification

Quantitative real-time PCR with SYBR green I detection (Applied Biosystems, Warrington, UK) was performed using a MyiQ Single-Color Real-Time PCR Detection System (Bio-Rad). Primers were designed using Primer Express Software (Applied Biosystems) and synthesized by Integrated DNA Technologies (Coralville, IA). Reactions were performed in a total volume of 25 µl including 12.5 µl 2 x Power SYBR Green PCR Master Mix (Qiagen, Valencia, CA), 1 µl 0.4 µM primer and 1 µl of the previously reverse-transcribed cDNA template. PCR cycling was performed using 96-well iCycler iQ PCR plates (Bio-Rad). PCR amplifications were performed for 45 cycles in which the initial 10 min denaturation at 95 °C was followed by denaturation at 95 °C for 15 sec, annealing at 58 °C for 20 sec and elongation at 72 °C for 30 sec. *Beta actin gene* was used as an internal control housekeeping gene to normalize the expression of *Nrf2 gene*. The sequences of *Nrf2* and *Beta actin gene* primers are listed in Table 1. Cycle thresholds (Ct) for all experimental groups were obtained by a MyiQ Single-Color Real-Time PCR Detection System (Bio-Rad). Delta Ct values were obtained by subtracting the *Nrf2 gene* Ct value of each sample from the *beta actin gene* Ct value. The relative expression profiles of the *Nrf2* transcripts were calculated using the $2^{-\Delta\Delta Ct}$ formula and recorded as fold changes (Rao et al. 2013). The specificity of *Nrf2* and *beta actin* qRT-PCR products were confirmed by melting curve analysis.

Table 1. Sequence of primers.

Gene	Primer	Primer sequence (5′-3′)	Product size (bp)
Nrf2 (Nfe2l2)	Forward	CGAGATATACGCAGGAGAGGTAAGA	79
	Reverse	GCTCGACAATGTTCTCCAGCTT	
Beta-actin (Actb)	Forward	TGCGTGACATCAAAGAGAAG	244
	Reverse	CGGATGTCAACGTCACACTT	

Statistical analysis

Data are means ± SD. Data were analyzed using Prism v 6.01 software (GraphPad San Diego, CA). Statistical analyses were performed using one-way ANOVA tests followed by *post hoc* Tukey tests. Values for $p \leq 0.05$ were considered statistically significant.

Results

Immunohistochemistry

We observed Nrf2 immunostaining in the luminal epithelium, glandular epithelium, stroma and myometrium of uteri and implantation sites. Nrf2 immunolocalization was uniformly cytoplasmic.

On days 1, 5 and 6 of pregnancy, Nrf2 expression was increased significantly compared to group C and groups D4 and D8 (Figures 1–3). We found no significant differences in Nrf2 expression among groups D1, D5 and D6 (Figure 3) nor among group C and groups D4 and D8 (Figure 3). We observed Nrf2 immunostaining in the luminal and glandular epithelium of group C. Nrf2 staining was weakly positive in the stroma and myometrium of group C (Figure 1B, C). For group D1, Nrf2 staining was localized mainly in the luminal epithelium, glandular epithelium and myometrium

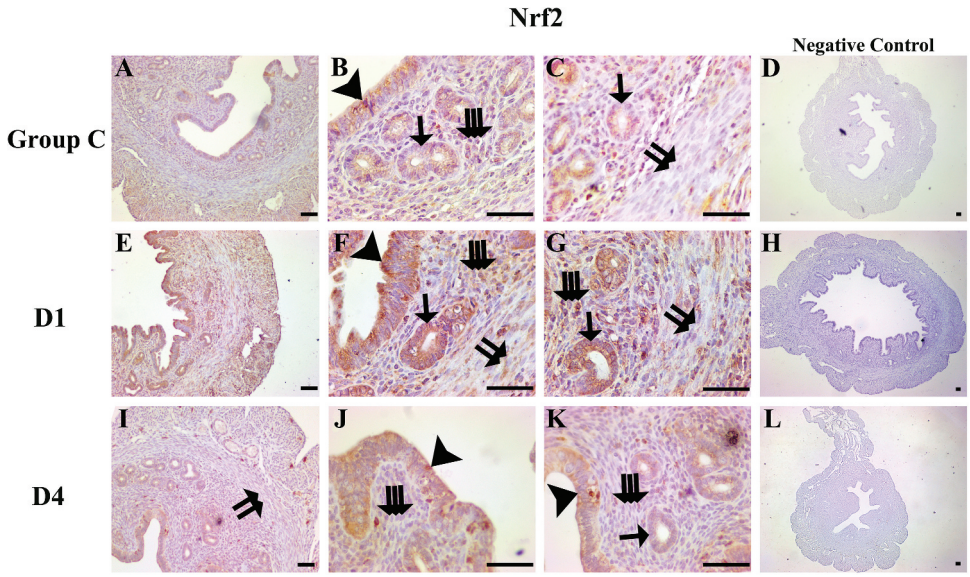

Figure 1. Nrf2 immunostaining in mouse uterus. A–D) Group C. E–H) D1 group. I–L) D4 group. Arrowhead, luminal epithelium; single arrow, glandular epithelium; double arrows, myometrial cells; triple arrows, stromal cells. Scale bars = 50 µm.

(Figure 1F, G). Strong Nrf2 immunostaining was observed in the luminal and glandular epithelium, but staining was weak in the stroma and (Figure 1G). Staining intensities in immunostained areas were classified as: weak, in pale staining; strong, intense staining and very strong, very intensely stained. In group D4, Nrf2 expression was decreased significantly in the luminal epithelium, glandular epithelium, stroma and myometrium

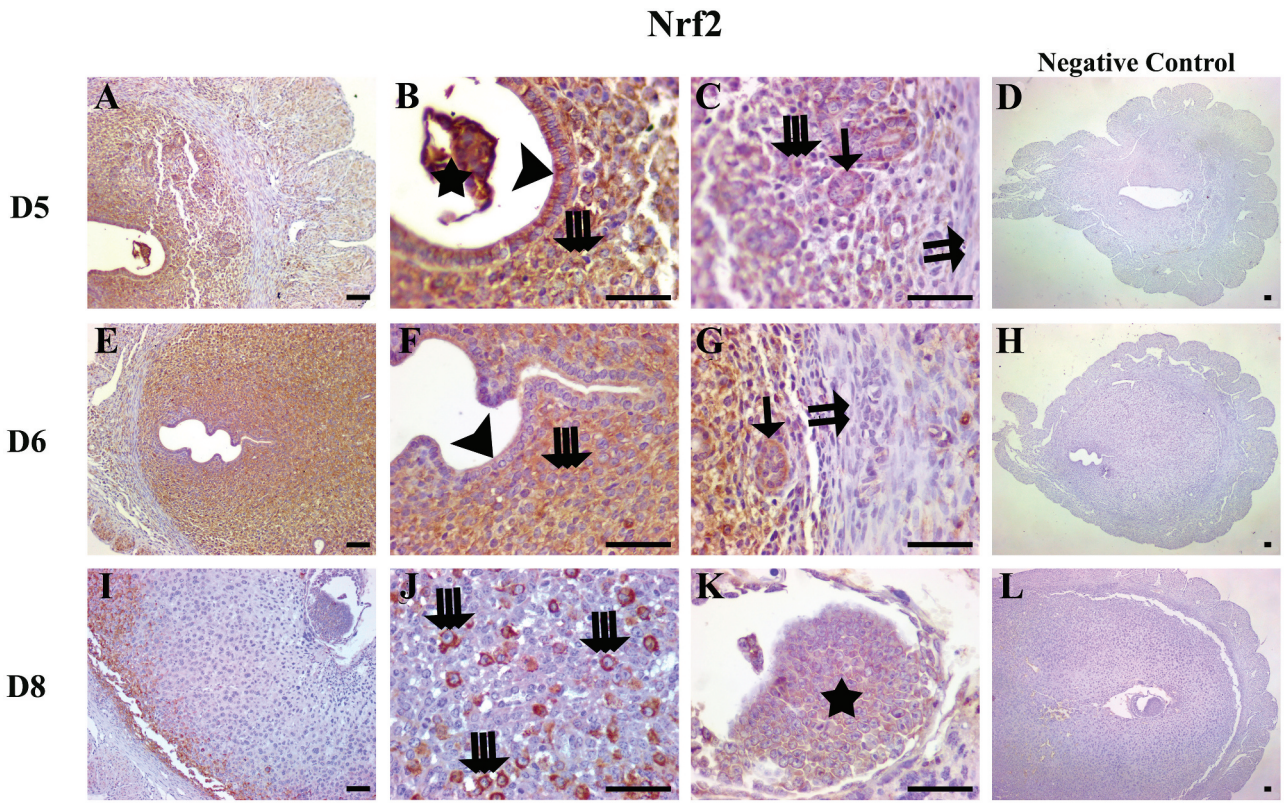

Figure 2. Nrf2 immunostaining of mouse implantation sites. A–D) D5 group. E–H) D6 group. I–L) D 8 group. Arrowhead, luminal epithelium; single arrow, glandular epithelium; Double arrows, myometrium cells; triple arrows, stromal cells; star, embryo. Scale bars = 50 µm.

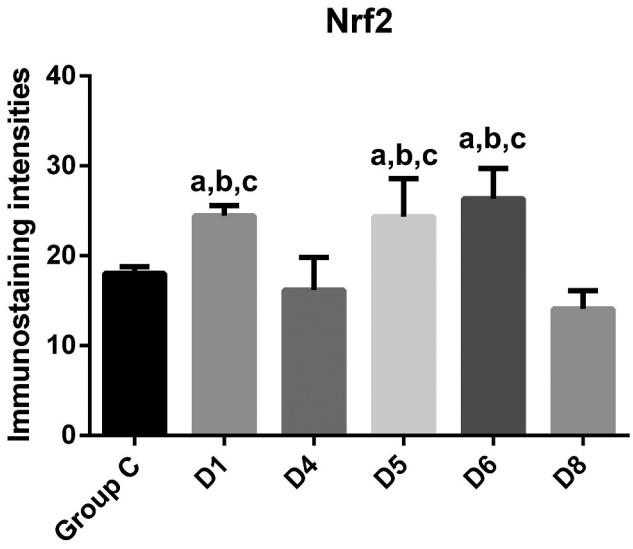

Figure 3. Nrf2 immunostaining for group C and groups D1, D4, D5, D6 and D8. Superscripts a – c indicate that values were significantly different compared to group C, D4 and D8 groups, respectively.

compared to group D1 (Figure 1J, K). In group D5, Nrf2 expression was increased significantly compared to group D4 and immunostaining was strong in the luminal epithelium and developing PDZ; weak Nrf2 immunostaining was observed in the glandular epithelium and myometrium (Figure 2B, C). Nrf2 staining was strong for group D4. For group D6, Nrf2 immunostaining was found in the luminal and glandular epithelium; it was very strong in the PDZ and SDZ (Figure 2F, G). Also for group D6, myometrium immunostaining was weak. For group D8, Nrf2 immunostaining was absent in the SDZ, but was very strong in cells between the myometrium and stroma. We found weak reactivity in the myometrium and embryo (Figure 2I–K).

Western blot

Nrf2 western blot results were consistent with Nrf2 immunohistochemistry findings. Nrf2 protein levels were increased significantly in groups D1, D5 and D6 compared to group C ($p < 0.05$) (Figure 4). The Nrf2 protein level was similar to group C for groups D4 and D8 (Figure 4). Also, for groups D1 and D5, Nrf2 expression was increased significantly compared to group D4 ($p < 0.05$) (Figure 4); however, we found no significant difference among groups D1, D5 and D6 (Figure 4).

Quantitative real-time PCR

Nrf2 mRNA expression for groups D1, D4 and D6 was not significantly different from group C (Figure 5). For groups D5 and D8, *Nrf2* mRNA expression was increased significantly compared to group C ($p < 0.05$) (Figure 5). We found no significant differences among groups D1, D4, D5, D6 and D8 (Figure 5).

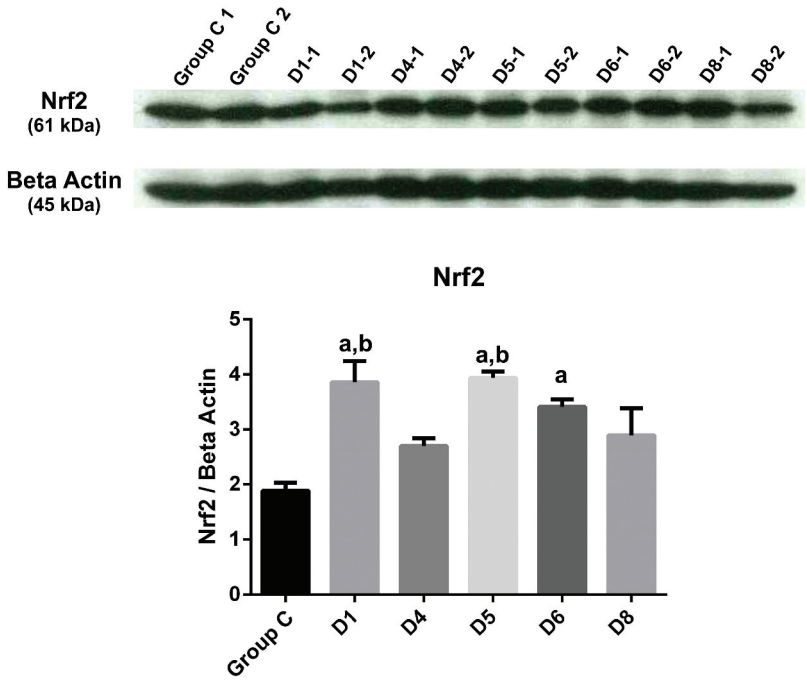

Figure 4. Nrf2 and beta actin western blot for group C and groups D1, D4, D5, D6 and D8. Beta actin was used as an internal control. Superscripts a and b indicate that these values were significantly different compared to group C and D4 group, respectively.

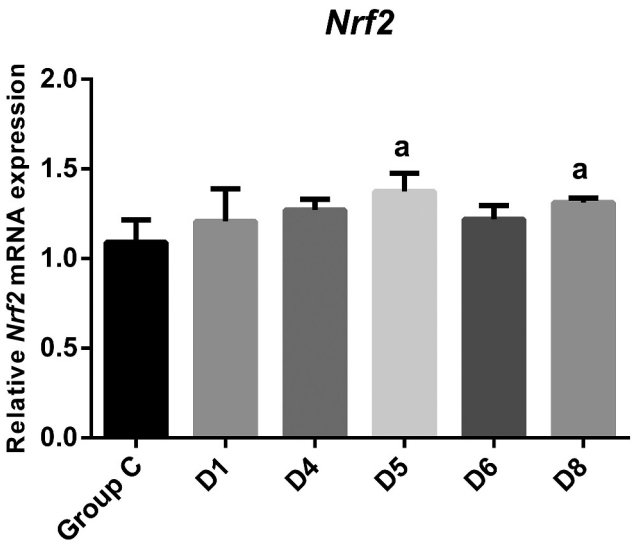

Figure 5. Relative levels of *Nrf2* transcripts for group C and groups D1, D4, D5, D6 and D8. Superscript indicates the value was significantly different compared to group C.

Discussion

We found that Nrf2 expression was increased significantly for groups D1, D5 and D6 compared to group C, but not for groups D4 and D8. For group D1, Nrf2 expression was increased in the stroma, and luminal and glandular epithelium compared to group C. Cheng et al. (2013) reported that Nrf2 plays an important role in protecting the fetus from oxidative stress in the uterus. Antioxidant enzyme systems in the female reproductive system are important for implantation and embryonic development (Blomberg et al. 2005; Al-Gubory et al. 2010). Consistent with earlier reports, we found that Nrf2 reduced oxidative stress and protected the fetus *in utero* in group D1.

The increased Nrf2 expression for group D1 was not observed for group D4. Increased Nrf2 expression on day 1 of pregnancy may activate the mechanisms required for ROS suppression so that Nrf2 expression is not required on day 4 of pregnancy. Laloraya et al. (1989a, 1989b) reported that high levels of superoxide anion in the implantation sites of group D5 mice reflects a possible role for this radical in vascular permeability when implantation is initiated. Our findings suggest that increased Nrf2 expression might counteract the adverse effects of ROS that are required for vascular permeability for implantation on day 5 of pregnancy. Dennery (2007) reported that antioxidant control of ROS is important for cellular signaling pathways involved in proliferation, differentiation and apoptosis during development. This investigator postulated that ROS induced oxidative stress can alter embryonic development. Ongoing implantation and embryonic development may produce excess ROS on day 6 of pregnancy.

Oxidative stress caused by excess ROS can affect embryonic development and implantation adversely. Therefore, increased Nrf2 expression may mitigate excess ROS on day 6 of pregnancy. After the blastocyst attaches to the implantation site in mice, decidualization begins in the stromal cells in that region (Parr et al. 1988). On day 5, the epithelioid and avascular PDZ is formed around the blastocyst (Paria et al. 1999). By day 6, stromal cells adjecent to the PDZ proliferate and differentiate into polyploid decidual cells to form the SDZ. SDZ development is completed on day 7 of pregnancy. By day 8 of pregnancy, the PDZ gradually begins to degenerate (Das 2010). Therefore, increased Nrf2 expression on days 5 and 6 of pregnancy may be related to removal of free radicals that are formed during the development of the PDZ and SDZ. Decreased Nrf2 expression on day 8 compared to days 5 and 6 of pregnancy may be related to decreased need for Nrf2 due to the completion of decidualization.

We investigated localization and expression of the antioxidant regulator protein, Nrf2, in uteri at estrus and on days 1 and 4 of pregnancy in mice, and in implantation sites on days 5, 6 and 8 in pregnant mice. Nrf2 may protect the developing embryo and the receptive uterine endometrium from the adverse effects of oxidative stress.

Disclosure statement

The authors declare no conflict of interest.

Funding

This work was supported by The Scientific and Technological Research Council of Turkey (TUBITAK), grant no. 213S032.

ORCID

Nuray Acar http://orcid.org/0000-0003-2531-0788

References

Acar N, Parlak H, Ozkan A, Soylu H, Avci S, Ustunel I, Izgut-Uysal VN, Agar A. 2019. The effect of docosahexanoic acid on apelin distribution of nervous system in the experimental mouse model of Parkinson's disease. Tissue Cell. 56:41–51. doi:10.1016/j.tice.2018.12.002.

Al-Gubory KH, Fowler PA, Garrel C. 2010. The roles of cellular reactive oxygen species, oxidative stress and antioxidants in pregnancy outcomes. Int J Biochem Cell Biol. 42:1634–1650. doi:10.1016/j.biocel.2010.06.001.

Bischof P, Campana A. 1997. Trophoblast differentiation and invasion: its significance for human embryo implantation. Early Preg Biol Med. 3:81–95.

Blomberg LA, Long EL, Sonstegard TS, Van Tassell CP, Dobrinsky JR, Zuelke KA. 2005. Serial analysis of gene expression during elongation of the peri-implantation porcine trophectoderm (conceptus). Physiol Genom. 20:188–194. doi:10.1152/physiolgenomics.00157.2004.

Cha J, Sun X, Dey SK. 2012. Mechanisms of implantation: strategies for successful pregnancy. Nat Med. 18:1754–1767. doi:10.1038/nm.3012.

Cheng X, Chapple SJ, Patel B, Puszyk W, Sugden D, Yin X, Mayr M, Siow RC, Mann GE. 2013. Gestational diabetes mellitus impairs Nrf2-mediated adaptive antioxidant defenses and redox signaling in fetal endothelial cells in utero. Diabetes. 62:4088–4097. doi:10.2337/db13-0169.

Das SK. 2010. Regional development of uterine decidualization: molecular signaling by Hoxa-10. Mol Reprod Dev. 77:387–396. doi:10.1002/mrd.21133.

Das SK, Wang XN, Paria BC, Damm D, Abraham JA, Klagsbrun M, Andrews GK, Dey SK. 1994. Heparin-Binding EGF-like growth factor gene is induced in the mouse uterus temporally by the blastocyst solely at the site of its apposition: a possible ligand for interaction with blastocyst EGF-receptor in implantation. Development. 120:1071–1083. doi:10.1242/dev.120.5.1071.

Dennery PA. 2007. Effects of oxidative stress on embryonic development. Birth Def Res Emb Today. 81:155–162. doi:10.1002/bdrc.20098.

Dey SK, Lim H, Das SK, Reese J, Paria BC, Daikoku T, Wang H. 2004. Molecular cues to implantation. Endocr Rev. 25:341–373. doi:10.1210/er.2003-0020.

Enders ACS. 1967. A morphological analysis of the early implantation stages in the rat. Am J Anat. 120:185–226. doi:10.1002/aja.1001200202.

Enders AC, Schlafke S. 1969. Cytological aspects of trophoblast-uterine interaction in early implantation. Am J Anat. 125:1–29. doi:10.1002/aja.1001250102.

Huet YM, Dey SK. 1987. Role of early and late oestrogenic effects on implantation in the mouse. J Reprod Fert. 81:453–458. doi:10.1530/jrf.0.0810453.

Huet-Hudson YM, Andrews GK, Dey SK. 1989. Cell type-specific localization of c-myc protein in the mouse uterus: modulation by steroid hormones and analysis of the peri-implantation period. Endocrinology. 125:1683–1690. doi:10.1210/endo-125-3-1683.

Ikeda H, Nishi S, Sakai M. 2004. Transcription factor Nrf2/MafK regulates rat placental glutathione S-transferase gene during hepatocarcinogenesis. Biochem J. 380:515–521. doi:10.1042/bj20031948.

Itoh K, Wakabayashi N, Katoh Y, Ishii T, Igarashi K, Engel JD, Yamamoto M. 1999. Keap1 represses nuclear activation of antioxidant responsive elements by Nrf2 through binding to the amino-terminal Neh2 domain. Genes Dev. 13:76–86. doi:10.1101/gad.13.1.76.

Jain S, Saxena D, Kumar GP, Laloraya M. 2000. NADPH dependent superoxide generation in the ovary and uterus of mice during estrous cycle and early pregnancy. Life Sci. 66:1139–1146. doi:10.1016/S0024-3205(00)00417-3.

Kaspar JW, Niture SK, Jaiswal AK. 2009. Nrf2:inrf2 (Keap1) signaling in oxidative stress. Free Rad Biol Med. 47:1304–1309. doi:10.1016/j.freeradbiomed.2009.07.035.

Kwak MK, Cho JM, Huang B, Shin S, Kensler TW. 2007. Role of increased expression of the proteasome in the protective effects of sulforaphane against hydrogen peroxide-mediated cytotoxicity in murine neuroblastoma cells. Free Rad Biol Med. 43:809–817. doi:10.1016/j.freeradbiomed.2007.05.029.

Laloraya M, Kumar GP, Laloraya MM. 1989a. Histochemical study of superoxide dismutase in the ovary of the rat during the oestrous cycle. J Reprod Fert. 86:583–587. doi:10.1530/jrf.0.0860583.

Laloraya M, Kumar GP, Laloraya MM. 1989b. A possible role of superoxide anion radical in the process of blastocyst implantation in *Mus musculus*. Biochem Biophys Res Commun. 161:762–770. doi:10.1016/0006-291X(89)92665-X.

Lee JS, Surh YJ. 2005. Nrf2 as a novel molecular target for chemoprevention. Cancer Lett. 224:171–184. doi:10.1016/j.canlet.2004.09.042.

Martin L, Finn CA. 1968. Hormonal regulation of cell division in epithelial and connective tissues of the mouse uterus. J Endocrinol. 41:363–371. doi:10.1677/joe.0.0410363.

Paria BC, Huet-Hudson YM, Dey SK. 1993. Blastocyst's state of activity determines the "window" of implantation in the receptive mouse uterus. Proc Natl Acad Sci USA. 90:10159–10162. doi:10.1073/pnas.90.21.10159.

Paria BC, Zhao X, Das SK, Dey SK, Yoshinaga K. 1999. Zonula occludens-1 and E-cadherin are coordinately expressed in the mouse uterus with the initiation of implantation and decidualization. Dev Biol. 208:488–501. doi:10.1006/dbio.1999.9206.

Parr MB, Parr EL, Munaretto K, Clark MR, Dey SK. 1988. Immunohistochemical localization of prostaglandin synthase in the rat uterus and embryo during the peri-implantation period. Biol Reprod. 38:333–343. doi:10.1095/biolreprod38.2.333.

Psychoyos A. 1973. Endocrine control of egg implantation. In: Greep R; Astwood A, and Geiger S, Eds., Handbook of physiology. American Physiological Society, Washington, DC; p. 187–215.

Ramos-Gomez M, Kwak MK, Dolan PM, Itoh K, Yamamoto M, Talalay P, Kensler TW. 2001. Sensitivity to carcinogenesis is increased and chemoprotective efficacy of enzyme inducers is lost in nrf2 transcription factor-deficient mice. Proc Natl Acad Sci USA. 98:3410–3415. doi:10.1073/pnas.051618798.

Rao X, Huang X, Zhou Z, Lin X. 2013. An improvement of the 2ˆ(-delta delta CT) method for quantitative real-time polymerase chain reaction data analysis. Biostat Bioinforma Biomath. 3:71–85.

Riley JC, Behrman HR. 1991. Oxygen radicals and reactive oxygen species in reproduction. Proc Soc Exp Biol Med. 198:781–791. doi:10.3181/00379727-198-43321C.

Rojo de la Vega M, Chapman E, Zhang DD. 2018. NRF2 and the hallmarks of cancer. Cancer Cell. 34:21–43. doi:10.1016/j.ccell.2018.03.022.

Ruder EH, Hartman TJ, Goldman MB. 2009. Impact of oxidative stress on female fertility. Curr Opin Obstet Gyn. 21:219–222. doi:10.1097/GCO.0b013e32832924ba.

Wang H, Dey SK. 2006. Roadmap to embryo implantation: clues from mouse models. Nat Rev Genet. 7:185–199. doi:10.1038/nrg1808.

Zhang DD. 2006. Mechanistic studies of the Nrf2-Keap1 signaling pathway. Drug Metab Rev. 38:769–789. doi:10.1080/03602530600971974.